Reshaping the folding energy landscape of human carbonic anhydrase II by a single point genetic mutation Pro237His

ARTICLE *in* THE INTERNATIONAL JOURNAL OF BIOCHEMISTRY & CELL BIOLOGY · FEBRUARY 2008

Impact Factor: 4.05 · DOI: 10.1016/j.biocel.2007.10.022 · Source: PubMed

6 AUTHORS, INCLUDING:

Jingtan Su
University of Southern California
12 PUBLICATIONS **66** CITATIONS
SEE PROFILE

Jun Zhang
Anhui University
892 PUBLICATIONS **13,768** CITATIONS
SEE PROFILE

Available online at www.sciencedirect.com
ScienceDirect
The International Journal of Biochemistry & Cell Biology 40 (2008) 776–788
IJBCB
www.elsevier.com/locate/biocel

Reshaping the folding energy landscape of human carbonic anhydrase II by a single point genetic mutation Pro237His

Yan Jiang [a,b,1], Jing-Tan Su [c,1], Jun Zhang [c,2], Xiang Wei [b], Yong-Bin Yan [c,*], Hai-Meng Zhou [b,**]

[a] *College of Life Sciences, Sichuan University, Chengdu 610064, Sichuan, PR China*
[b] *Protein Science Laboratory of the Ministry of Education, Department of Biological Sciences and Biotechnology, Tsinghua University, Beijing 100084, PR China*
[c] *State Key Laboratory of Biomembrane and Membrane Biotechnology, Department of Biological Sciences and Biotechnology, Tsinghua University, Beijing 100084, PR China*

Received 24 June 2007; received in revised form 3 September 2007; accepted 15 October 2007
Available online 24 October 2007

Abstract

Human carbonic anhydrase (HCA) II participates in a variety of important biological processes, and it has long been known that genetic mutations of HCA II are closely correlated to human disease. In this research, we investigated the effects of a genetic single point mutation P237, which is located on the surface of the molecule and does not participate in the HCA II catalysis, on HCA II activity, stability and folding. Spectroscopic studies revealed that the mutation caused more buried Trp residues to become accessible by solvent and caused the NMR signals to become less dispersed, but did not affect the secondary structure or the hydrophobic exposure of the protein. The mutant was less stable than the wild type enzyme against heat- and GdnHCl-induced inactivation, but its pH adaptation was similar to the wild type. The mutation slightly decreased the stability of the molten globular intermediate, but gradually affected the stability of the native state by a 10-fold reduction of the Gibbs free energy for the transition from the native state to the intermediate. This might have led to an accumulation of the aggregation-prone molten globular intermediate, which further trapped the proteins into the off-pathway aggregates during refolding and reduced the levels of active enzyme *in vivo*. The results herein suggested that the correct positioning of the long loop around P237 might be crucial to the folding of HCA II, particularly the formation of the active site.

Keywords: Protein aggregation; Human carbonic anhydrase II; Genetic mutation; Protein folding pathways; Molten globule

Abbreviations: ANS, 8-anilino-1-naphthalene sulfonic acid; CA, carbonic anhydrase; GdnHCl, guanidine hydrochloride; HCA, human carbonic anhydrase; CD, circular dichroism; I_{320}, intrinsic fluorescence intensity at 320 nm; I_{365}, intrinsic fluorescence intensity at 365 nm; IPTG, isopropyl-β,D-thiogalactopyranoside; *p*-NPA, *p*-nitrophenol acetate; SEC, size exclusion chromatography; WT, wild type.

* Corresponding author. Fax: +86 10 6277 1597.
** Corresponding author. Fax: +86 10 6277 2245.
E-mail addresses: ybyan@tsinghua.edu.cn (Y.-B. Yan), zhm-dbs@tsinghua.edu.cn (H.-M. Zhou).
[1] These authors contributed equally to this work.
[2] Present address: Department of Biochemistry and Biophysics, School of Medicine, University of North Carolina at Chapel Hill, Chapel Hill, NC 27599-7260, USA.

1357-2725/$ – see front matter © 2007 Elsevier Ltd. All rights reserved.
doi:10.1016/j.biocel.2007.10.022

1. Introduction

Anfinsen's thermodynamic hypothesis, which is thought to be the central pillar of protein science, states that the amino acid sequence determines the native three-dimensional structure of a protein in a state of thermodynamic equilibrium corresponding to the system with the lowest free energy (Anfinsen, 1973). The folding and the stability of proteins in physiological conditions are known to be closely correlated to their functions, and thus aberrant protein folding/unfolding may cause loss-of-function of proteins and even disease (Dobson, 2001, 2003). Although the problem of how the folding is encoded in the sequence is not fully understood, it is known that some disease-related genetic mutations can gradually alter the folding or the stability of proteins (for example, Almstedt et al., 2004; Feng, Zhao, Zhou, & Yan, 2007; Francis, Berry, Moore, & Bhattacharya, 1999; Stefani & Dobson, 2003). Doubtless, knowledge of the biochemistry of disease-related mutations can provide invaluable information for understanding the mechanisms of these diseases and developing new therapies for them.

Human carbonic anhydrase (HCA) II, which belongs to a large zinc metalloenzyme family, catalyzes the reversible hydration of carbon dioxide (Lindskog, 1997). Its evolutionarily homologous forms have been found in most organisms from bacteria to human, and carbonic anhydrase (CA) appears to have an ancient lineage. As a model protein, the folding of CA has been well characterized as a multi-step process involving two intermediates (Bushmarina, Kuznetsova, Biktashev, Turoverov, & Uversky, 2001; Cleland & Wang, 1990; Henkens, Kitchell, Lottich, Stein, & Williams, 1982; Semisotnov et al., 1990; Wong & Tanford, 1973), in which the first but not the second refolding intermediate is prone to aggregate (Cleland & Wang, 1990; Jiang, Yan, & Zhou, 2006). As a vital enzyme for cell and body functions, CA participates in a variety of biological processes including respiration, calcification, acid–base balance, bone resorption, and the formation of aqueous humor, cerebrospinal fluid, saliva, and gastric acid (Dodgson, Tashian, Gross, & Carter, 1991). It has also long been known that genetic mutations of HCA II are closely correlated to several human diseases. About three decades ago, Sly et al. (1972) described three sisters with a form of osteopetrosis that was associated to HCA II mutation (Sly, Hewett-Emmett, Whyte, Yu, & Tashian, 1983). Since then, medical surveys have reported many CA II single point mutations such as Asn252Asp (Lin & Deutsch, 1972), Lys17Glu (Jones, Sofro, & Shaw, 1982), His107Tyr (Roth, Venta, Tashian, & Sly, 1992; Venta, Welty, Johnson, Sly, & Tashian, 1991), Tyr40Ter (Soda, Yukizane, Yoshida, Aramaki, & Kato, 1995), and the deletion of a single cytosine in codon 207 (Borthwick et al., 2003). Some of these mutations are thought to cause deficiencies and are regarded as the primary cause of an inherited syndrome of osteopetrosis with renal tubular acidosis and cerebral calcification (Hu, Lim, Ciccolella, Strisciuglio, & Sly, 1997; Sly & Hu, 1995). It has also been found that the disease-related mutations discovered in HCA II defects usually can be addressed as conformational diseases (Almstedt et al., 2004).

In 1983, one more single amino acid substitution Pro237His of HCA II (HCA II_{P237H}) was discovered in a Caucasian woman by screening of hemolysate (Jones & Shaw, 1983). This variant was reported to have similar enzyme activity but less heat stability when compared with the WT HCA II. However, only subjects heterozygous for this mutation have been found, and the lack of knowledge of how this mutation affects the structure and folding of HCA II makes it difficult to understand how this single point mutation leads to disease. According to the structure of HCA II (Hakansson, Carlsson, Svensson, & Liljas, 1992), Pro237 is located on the surface of the molecule and does not participate in the substrate binding or catalysis of the enzyme (Fig. 1). In this research, the P237H mutation was found to gradually destabilize the enzyme and affect the folding pathway of HCA II. These findings provide clues in understanding how this mutation causes loss-of-function folding disease *in vivo*. Moreover, the results herein also contribute to understanding the mechanisms of the folding of the model protein HCA II.

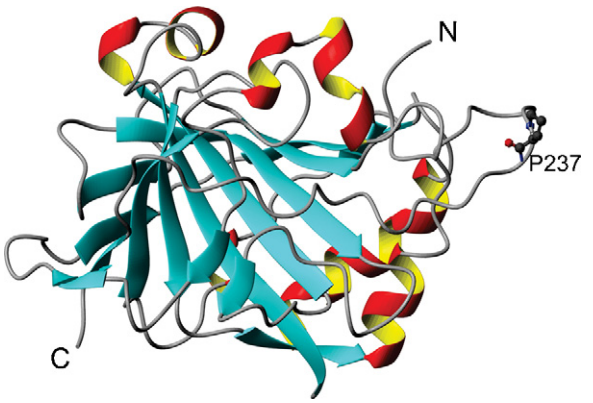

Fig. 1. Schematic structure of HCA II from PDB coordinates 2CBA. The location of P237 is highlighted by the ball-and-stick model. N and C denote the N- and C-terminus.

2. Materials and methods

2.1. Materials

Ultra pure guanidine hydrochloride (GdnHCl), Tris base, sulfuric acid, *p*-nitrophenol acetate (*p*-NPA), 8-anilino-1-naphthalene sulfonic acid (ANS), isopropyl-β,D-thiogalactopyranoside (IPTG) and diethylpyrocarbonate (DEPC) were purchased from Sigma–Aldrich Inc. (St. Louis, MO, USA). All other chemicals were analytical grade from local distributors. All buffers and protein solutions were prepared by using ultrapure water from a MilliQ water purification system (Millipore Corp., Bedford, MA, USA).

2.2. Expression and purification of wild type and P237H HCA II

The wild type (WT) HCA II gene full ORF clone IOH1900 was purchased from Invitrogen (Invitrogen Corp, Carlsbad, CA, USA). Site-directed mutagenesis was performed by overlap extension using the WT HCA II gene as a template. The WT and mutated HCA II gene were cloned into the expression vector pET28b. The proteins were overexpressed in *E. coli* strain BL21 (λDE3) grown in LB broth with 50 μg/mL Kanamycin, at 37 °C to a cell density corresponding to $A_{600\,nm} = 0.5$. The culture temperature was then dropped to 20 °C. The protein production was initiated by adding 0.5 mM IPTG and $ZnSO_4$. Bacterial cells were sonicated and the enzyme was purified by Ni^{2+}-NTA affinity chromatography and further purified by size exclusion chromatography (SEC) performed on a Superdex 200 HR 10/30 column attached to an AKTA purifier (Amersham Pharmacia Biotech, Sweden). The protein concentration was determined by measuring the absorbance at 280 nm using $\varepsilon_{280\,nm} = 53{,}800\,M^{-1}\,cm^{-1}$.

2.3. Aggregation measurements

The aggregation experiments were carried out at 25 °C by rapid dilution of GdnHCl-denatured WT and P237H HCA II into the Tris-sulfate buffer. The final concentration of the protein was 10 μM. The turbidity was monitored by measuring the light absorbance at 400 nm with an Ultraspec 4300 pro UV/Visible spectrophotometer from Amersham Pharmacia Biotech (Uppsala, Sweden).

2.4. Activity assay

The HCA II activity was determined by using the esterase activity assay, which monitors the appearance of *p*-nitrophenolate anion spectrophotometrically during the hydrolysis of *p*-NPA by HCA II (Pocker & Stone, 1967). In brief, the substrate stock solution was prepared by dissolving *p*-NPA in acetonitrile with a concentration of 3 mM. The esterase activity of HCA II was measured at 4 °C or 25 °C by the addition of 200 μL of the substrate solution to 600 μL reaction buffer. Then the rate of increase in absorbance at 400 nm was measured. The enzymatic parameters K_m and V_{max} of the WT and P237H HCA II were measured with the final enzyme concentration of 1.5 μM using different concentrations of *p*-NPA in a 15 mM Tris-sulfate (pH 7.5) system at 4 °C. The different concentrations of substrate and the measured activity were plotted by the Lineweaver–Burk double-reciprocal method. V_{max} and K_m were deduced from the slopes and intercepts of these plots.

2.5. Stability

The stability against GdnHCl denaturation was evaluated by the residual activity of the samples. The samples were prepared by inactivating 3 μM WT or P237H HCA II in 15 mM Tris-sulfate buffer (pH 7.5) containing different concentrations of GdnHCl at 25 °C for 6 h. Then the residual activity of each sample was measured by the esterase activity assay. The activity of the WT HCA II without the addition of GdnHCl was taken as 100% to normalize the data.

As for the thermal stability measurements, 3 μM of the enzymes in 15 mM Tris-sulfate buffer (pH 7.5) were incubated in a thermostatic cell for 1 h. Then the samples were cooled to 25 °C, and the residual activities were measured at 25 °C. The activity of the WT enzyme equilibrated at 25 °C was taken as 100% to normalize the data.

The pH adaptation of the enzyme was measured by adjusting the pH from 10.0 to 8.0 (in phosphate-buffered saline) and 8.0 to 5.5 (in Tris-sulfate buffer) using H_2SO_4. The solutions were equilibrated at 25 °C for 12 h. The pH value of each solution was re-checked before the activity assay. The activity of the WT enzyme measured at pH 10.0 was taken as 100% to normalize the data.

2.6. Unfolding and refolding measurements

The WT and P237H HCA II (1.5 μM in 100 mM Tris-sulfate, pH 7.5) were incubated at 25 °C in various concentrations of GdnHCl for 6 h to prepare the samples for the unfolding experiments. The refolding experiments were prepared by diluting the 5 M GdnHCl-denatured WT and mutated proteins into 100 mM

Tris-sulfate buffer containing certain concentrations of GdnHCl at a mixing ratio of 1:100 and equilibrated for 6 h before measurement. The final protein concentration was 1.5 μM. The intrinsic tryptophan fluorescence of each solution was measured on an F-2500 fluorescence spectrophotometer (Hitachi Ltd., Tokyo, Japan). The excitation wavelength was 296 nm and the emission spectra were recorded in the wavelength region of 300–400 nm. Both entrance and exit slit widths were set to 5 nm.

ANS was added to the unfolding or refolding samples with a final concentration of 75 μM. After an additional 30 min incubation, the ANS spectra were measured by excitation at 350 nm, and then emission spectra were recorded in the wavelength region of 400–600 nm. The fluorescence intensity at 480 nm was plotted as a function of the GdnHCl concentrations to reflect the change in hydrophobic exposure of the samples.

The phase diagram treatment of the intrinsic fluorescence data is a sensitive way to detect the unfolding intermediates and was carried out as described previously (Bushmarina et al., 2001; Su, Kim, & Yan, 2007). In brief, the fluorescence intensities at 320 and 365 nm were used to characterize the position and form of the fluorescence spectra by the parameter $A = I_{320}/I_{365}$, where I_{320} and I_{365} are the fluorescence intensities at $\lambda_{em} = 320$ and 365, respectively. The fluorescence intensities at 320 and 365 nm of the native state were used to normalize the data. The "phase diagram" was constructed using I_{320} versus I_{365} under different experimental conditions for the WT and mutated HCA II undergoing structural transitions.

2.7. Structural simulations

The structural simulations were carried out using the Tripos molecular modeling software SYBYL version 6.3. The HCA II crystal structure (PDB ID 2CBA) was used for the homology modeling of the structure of the mutated protein. The molecular dynamics simulation was carried out with a time range of 1000 fs and a step of 1 fs at a temperature of 300 K under the Tripos force field. The hydrogen bond analysis of the local structure was performed by using UCSF Chimera beta version 1 with the relaxed H-bond constraints of 0.4 Å and 20.0°.

2.8. CD and NMR measurements

The far-UV circular dichroism (CD) spectra were recorded on a Jasco-715 spectrophotometer (Tokyo, Japan) over a wavelength range of 190–250 nm using 0.1-cm-pathlength cells. The final protein concentration for CD experiments was 1.5 μM. The presented spectra are the average of three repetitions. The ^{1}H NMR experiments were performed on a Varian Unity Inova 500NB NMR spectrometer equipped with three RF channels and a triple-resonance pulsed-field gradient probe. The NMR samples were prepared by concentrating the WT and P237H HCA II proteins to a final concentration of 0.1 mM in Tris-SO_4 buffer, pH 7.5. The solutions were centrifuged at 6000 × *g* for 10 min to remove possible insoluble proteins, and then about 500 μL solutions containing 10% D_2O were transferred to a 5 mm NMR tube. One-dimensional ^{1}H spectra were collected at 22 °C with a spectral width of 8003.2 Hz (16 ppm), 128 repetitions, a recycle delay of 1 s, and an acquisition time of 1 s. The chemical shifts were referenced to the ^1H_2O resonance set to 4.7 ppm. All NMR data were processed and analyzed by using the VNMR software provided by Varian Inc.

3. Results

3.1. Effect of P237H mutation on HCA II activity and structure

The activities and enzymatic parameters K_m and V_{max} of native wild type (WT) and mutated HCA II were determined by esterase activity assay at 4 °C. The WT and P237H HCA II dependence of the enzymatic rate on substrate concentration follows the classical Michaelis–Menten relationship. Thus the Lineweaver–Burk plot at a constant enzyme concentration was used to obtain the enzymatic parameters K_m and V_{max} (Fig. 2). Although P237 does not participate in

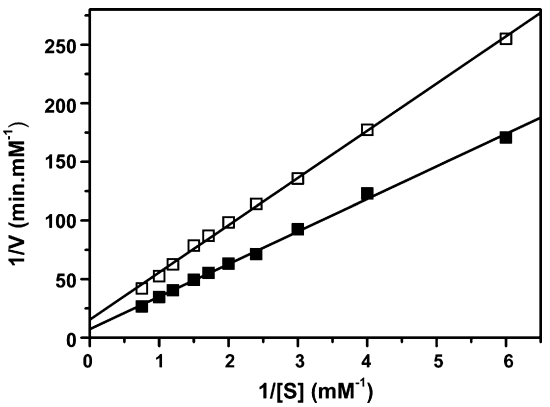

Fig. 2. Lineweaver–Burk plots for esterase activity of the wild type (filled squares) and P237H (open squares) HCA II. Experiments were carried out at 4 °C. The enzymatic parameters obtained are presented in Table 1. The substrate used for the assay was *p*-NPA, *V* is the reaction velocity and [S] is the substrate concentration, respectively.

Table 1
Enzymatic and stability parameters of the wild type and P237H HCA II

	K_m (mM)	V_{max} (mM/min)	ΔG_{NI}° (kcal/mol)	ΔG_{IU}° (kcal/mol)	$T_{1/2}$ (°C)	Unfolding intermediate [GdnHCl] (M)	Refolding intermediate [GdnHCl] (M)
WT	2.6 ± 0.3	0.14 ± 0.02	4.8 ± 0.2	10.4 ± 0.8	54.3 ± 0.3	1.4, 1.8	1.1
P237H	4.0 ± 0.8	0.07 ± 0.01	0.5 ± 0.2	7.4 ± 0.3	43.1 ± 0.6	0.2, 0.4, 1.4	1.4

the substrate binding and the catalysis of HCA II, it was found that P237H mutation decreased the esterase activity of HCA II to about 50% of that of the WT enzyme. Furthermore, the value of K_m was increased about 50% by the P237H mutation, while the maximum catalytic rate V_{max} was about 45% of the WT. These results suggested that the P237H mutation might decrease the activity by affecting the structure of HCA II. The K_m values in Table 1 were similar to those previously reported (Jones & Shaw, 1983), whereas the V_{max} values and relative activity were slower than in the previous reports. This different observation might be caused by the dissimilar origins of the proteins were used in the research. The previous report used proteins purified directly from the red cells of the patients, whereas recombinant proteins were used in this research.

To further investigate the effects of P237H mutation on the tertiary structure of HCA II, CD, NMR, intrinsic Trp fluorescence and ANS fluorescence spectra were measured (Fig. 3). The CD spectra of the two proteins were similar, while the mean residue ellipticity of the mutated protein was slightly smaller than the WT protein. This suggested that the mutation might have minor effects on HCA II secondary structures. The microenvironments of the Trp residues were affected by the mutation as revealed by a red-shift of the emission maximum of the Trp fluorescence (from 331 to 334.5 nm). Meanwhile, no significant difference was observed in the ANS spectra of the WT and mutated enzymes, which indicated that the P237H mutation did not affect the hydrophobic exposure of the HCA II. The NMR spectrum of the mutated protein was also similar to the WT protein. However, the NMR signals of the WT protein were more dispersed than the P237H HCA II, particularly those between −1 and 2 ppm and between 7.5 and 11 ppm. The lower dispersion of the NMR spectrum indicated that the solution structure of the mutated protein was less structured than the WT protein.

3.2. Effect of P237H mutation on HCA II stability

WT HCA II is a relatively stable enzyme due to the binding of one zinc ion in the active site (Lindskog, 1997). To investigate whether the P237H mutation affects the stability of HCA II, the activity assay was used to monitor the stability against heat-, acid-, and GdnHCl-induced inactivation. The thermal stability of WT and P237H HCA II was determined by incubation of samples at specific temperatures for 1 h followed by the measurement of activity at 25 °C. As shown in Fig. 4A, the WT HCA II could retain its activity after heat treatment at 52 °C for 1 h, and totally lost its activity after treatment at 60 °C. The P237H mutant was dramatically more unstable at elevated temperatures than the WT enzyme. The activity of P237H HCA II began to decrease after heat treatment at temperatures above 35 °C, a temperature close to physiological conditions. The midpoint of P237H HCA II thermal inactivation was about 40 °C, which is much lower than that of the WT enzyme (about 55 °C). This observation is consistent with the previous results (Jones & Shaw, 1983). Similar to the thermal inactivation results, P237H HCA II was less stable than the WT enzyme during the inactivation induced by GdnHCl (Fig. 4B). The WT enzyme lost most of its activity at GdnHCl concentrations above 1.0 M, whereas the mutant lost its activity when the GdnHCl concentration was higher than 0.4 M. Unlike the stability against thermal and GdnHCl denaturation, the acid and basic tolerance of the WT and mutant was almost the same from pH 5.5 to 10.0, although the activity of the mutant was only about 40% of that of the WT enzyme at each pH value. These results indicated that the P237H mutation gradually affected the stability of the HCA II active site against heat- and chemical-denaturation, but did not affect the stability against acid-denaturation.

3.3. Effect of P237H mutation on HCA II equilibrium unfolding and refolding

During the expression of the WT and mutated enzyme, inclusion bodies could be observed even though the expression temperature was reduced to 20 °C, while the yield of the soluble mutated proteins was much smaller than the WT enzyme as characterized by SDS-PAGE (data not shown). Since only a limited yield of the soluble P23H HCA II could be obtained in the super-

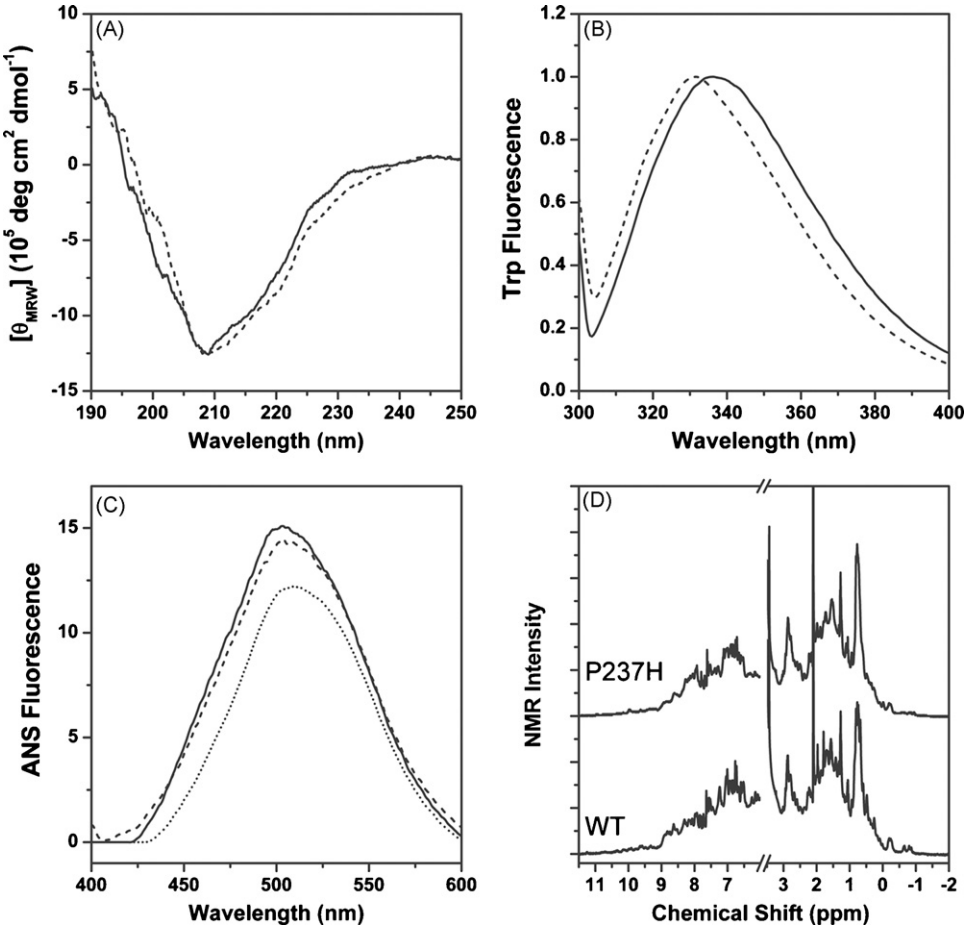

Fig. 3. Effects of P237H mutation on HCA II tertiary structure. (A) CD spectra of the wild type (dashed lines) and P237H (solid lines) HCA II. (B) Intrinsic Trp fluorescence spectra of the wild type (dashed lines) and P237H (solid lines) HCA II. The excitation wavelength was 296 nm. (C) ANS spectra of the wild type (dashed lines) and P237H (solid lines) HCA II. ANS (final concentration 75 μM) was added to the samples, and the ANS spectra were measured after 30 min incubation. The spectrum of the ANS background is also shown as dotted lines. (D) ^{1}H NMR spectra of the two proteins. The final protein concentration was 1.5 μM for the CD and fluorescence experiments, and 0.1 mM for NMR experiments.

natant, we also tried to refold the mutant *in vitro* by the dilution of P237H HCA II inclusion bodies solubilized in 8 M urea. However, no active enzymes of P237H HCA II could be obtained by the dilution method as monitored by activity assay, while the WT enzyme could be successfully reactivated by the same rapid dilution method. To explore whether the P237H mutation was more prone to form off-pathway aggregates during folding, the aggregation of GdnHCl-denatured protein after rapid dilution was measured by turbidity. Consistent with previous studies (Cleland & Wang, 1990; Wetlaufer & Xie, 1995), aggregation could be observed when the final protein concentration was above 10 μM in the direct-dilution experiments (Fig. 5). The results indicated that the aggregation of the mutant was much greater than that of the WT enzyme. Since the refolding of CA involves two intermediates and the first one is prone to aggregate (Cleland & Wang, 1990; Jiang et al., 2006), the results of the aggregation experiments suggested that the P237 mutation might affect the correct refolding of the first refolding intermediate of HCA II. To further confirm this hypothesis, equilibrium unfolding and refolding of WT and P237H HCA II were investigated by intrinsic and ANS fluorescence spectroscopy. To avoid the possible interference of aggregates on the fluorescence spectra, a final protein concentration of 1.5 μM was chosen in the folding studies. The turbidity at 400 nm indicated that at this concentration, neither the WT nor P23H HCA II would form insoluble aggregates during unfolding/refolding (data not shown).

The unfolding samples of the WT and P237H HCA II were prepared by dissolving the enzymes in buffers containing given concentrations of GdnHCl and incubated at 25 °C for 6 h. Consistent with previous studies

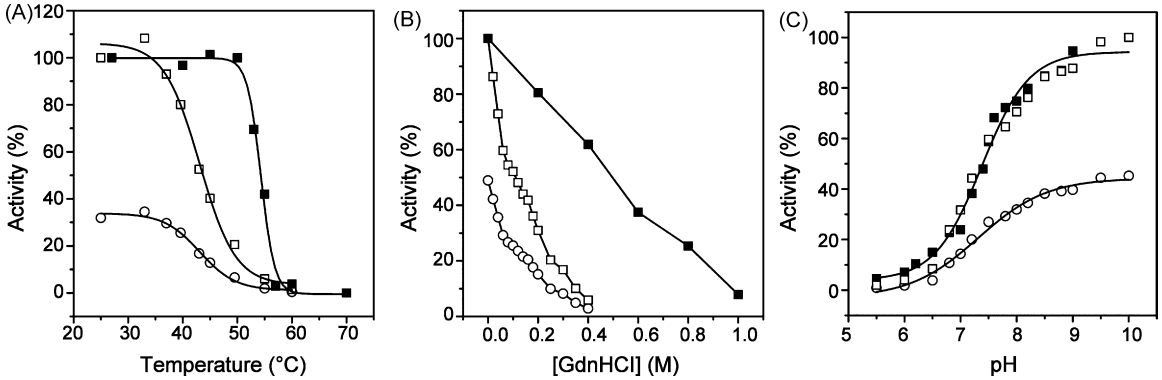

Fig. 4. Effects of P237H mutation on HCA II stability evaluated by the activity of the wild type (filled squares) and P237H HCA II (open squares and circles). (A) The thermal stability was measured by incubating the samples at a given temperature for 1 h and then the activities were measured at 25 °C. The data were normalized by the activities of the samples treated at 25 °C (squares) or the activity of the wild type HCA II at 25 °C (filled squares and open circles). (B) The stability against GdnHCl inactivation was measured by incubating the enzymes for 6 h in buffers containing given concentrations of GdnHCl. The GdnHCl-induced inactivation experiments were performed at 4 °C to avoid possible aggregation due to long-term incubation. The data were normalized by the activities of samples in the absence of GdnHCl (squares) or the activity of wild type HCA II at 4 °C (closed squares and open circles). (C) The pH adaptation of the WT (closed squares) and the mutated (open circles) enzyme was measured by adjusting the pH from 10.0 to 8.0 (in phosphate-buffered saline) and 8.0 to 5.5 (in Tris-sulfate buffer) using H_2SO_4. The solutions were equilibrated at 25 °C for 12 h. The activities at pH 10.0 were taken as 100% to normalize the data. The relative activities of P237H HCA II to the WT enzyme (open squares) were also shown by normalizing the data by the activity of WT HCA II at pH 10.0.

(Bushmarina et al., 2001; Cleland & Wang, 1990; Henkens et al., 1982; Semisotnov et al., 1990; Wong & Tanford, 1973), the equilibrium unfolding of WT HCA II was a three-state process with the population of a molten globule-like intermediate, which was characterized by the appearance of a plateau in the emission maximum wavelength of intrinsic fluorescence (E_{max}) and a peak in the ANS fluorescence intensity (Fig. 6A and B). The unfolding profile of the P237H HCA II indicated that the mutant had a similar three-state unfolding process, but was less stable than the WT. The first dramatic change of the E_{max} values was in buffers with about 0.6 M GdnHCl,

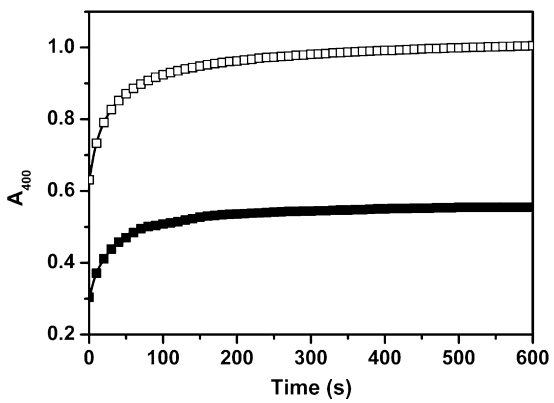

Fig. 5. Aggregation of the wild type (filled squares) and P237H (open squares) HCA II during refolding from the GdnHCl-denatured states by direct dilution. Aggregation was monitored by measuring the turbidity at 400 nm. The final protein concentration was 10 μM.

while that of the mutant was about 0.3 M GdnHCl. This result coincided with the inactivation results presented in Fig. 4B. The most interesting observation is that a much wider plateau of E_{max} (from 0.4 to 1.5 M GdnHCl) could be observed for the mutant compared to the WT protein. Consequently, the greatest ANS intensity of P237H HCAII appeared at a GdnHCl concentration (~1.0 M) lower than that of the WT protein (~1.6 M). The maximum intensities of the ANS fluorescence for the two proteins were similar, which suggested that P237H HCA II might form similar amounts of molten globule intermediates (similar hydrophobic exposures) to the WT protein. The E_{max} values of the mutant were found to be larger than those of the WT at most GdnHCl concentrations, which indicated that the Trp residues were more exposed to water. It is also worth noting that dissimilarity could also be observed for the transition from the intermediate to the unfolded states (from 1.5 to 3 M GdnHCl). The mutant's transition was much more steep than the WT's, and the mutant reached its unfolded state at a GdnHCl concentration of about 2.0 M. These results suggested that the intermediate of the P237H HCA II might be less stable than that of the WT. The Gibbs free energy of denaturation for the transitions from the native state (N) to the intermediate (I) and from I to the unfolded state (U) was calculated according to the method of linear extrapolation (Table 1) (Santoro & Bolen, 1988). The Gibbs free energy ΔG_{IU}° was slightly decreased (about 30% reduction) by the P237H mutation. However, the value $\Delta G_{NI}^{H_2O}$ was gradually affected by the mutation,

which was 4.8 ± 0.2 kcal/mol for the WT protein and 0.5 ± 0.2 kcal/mol for the mutant.

To investigate whether the refolding of the WT and P237H HCA II was reversible, the GdnHCl-denatured samples were refolded by dilution to buffers containing certain concentrations of GdnHCl and the refolding was monitored by intrinsic Trp and ANS fluorescence (Fig. 6C and D). The transition of the WT protein was similar to the unfolding curve, and a plateau between 1.4 and 1.8 M GdnHCl in the E_{max} curve and a peak at 1.4 M GdnHCl in the ANS fluorescence intensity curve could be observed. Both the E_{max} and ANS fluorescence intensity values were found to be able to recover to that of the native enzyme. These results indicated that the folding of WT HCA II was reversible under the conditions used in this research, which is consistent with previous studies (Cleland & Wang, 1990). The E_{max} curve for P237H HCA II refolding was also found to be similar to its unfolding curve. However, unlike the unfolding experiments, the maximum ANS fluorescence intensity of P237H HCA II was greater than that of the WT, which indicated that more hydrophobic exposure could be observed during the refolding of the mutant. The difference in ANS experiments between the two proteins also suggested that there might be more intermediates accumulated during the refolding of the mutated protein. Moreover, the mutant could not regain its native state since a discrepancy could be observed for the two samples at the lowest GdnHCl concentration.

3.4. Parameter A and phase diagram analysis

Parameter A, which is the quotient of the fluorescence intensity at 320 nm (I_{320}) to that at 365 nm (I_{365}), reflects the shape of a fluorescence spectrum (Turoverov, Haitlina, & Pinaev, 1976) and can be used to monitor the protein folding pathways. As shown in Fig. 7A, parameter A underwent similar sigmoidal transitions for the unfolding and refolding of the WT HCA II. The discrepancy of the parameter A values at GdnHCl concentrations from 0 to 2 M indicated that the folding of the WT HCA II was not fully reversible. As for the P237H HCA II, the transition curves (Fig. 7D) were quite different between unfolding and refolding,

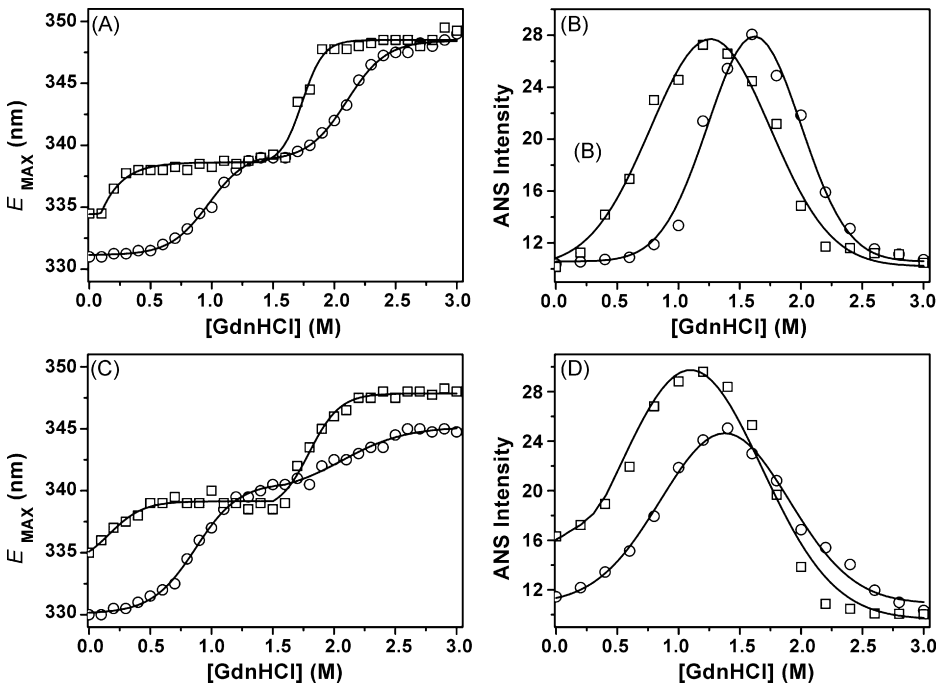

Fig. 6. Unfolding (A and B) and refolding (C and D) of the wild type (squares) and P237H (circles) HCA II A monitored by intrinsic Trp (A and C) and ANS fluorescence (B and D). The unfolding experiments were carried out by denaturing the enzymes in buffers containing various concentrations of GdnHCl at 25 °C for 6 h. The refolding samples were prepared by diluting the 5 M GdnHCl-denatured proteins into 100 mM Tris-sulfate buffer containing certain concentrations of GdnHCl at a mixing ratio of 1:100. The samples were equilibrated for 6 h before measurements. The final protein concentration was 1.5 μM. (A and C) The unfolding was evaluated by the change of the emission maximum wavelength (E_{max}) of the Trp fluorescence spectra. (B and D) The transition was monitored by the intensity of the ANS fluorescence at 480 nm with an excitation at 350 nm. The final ANS concentration was 75 μM. ANS was added to the unfolding/refolding samples, and the spectra were measured after a further 30 min equilibration.

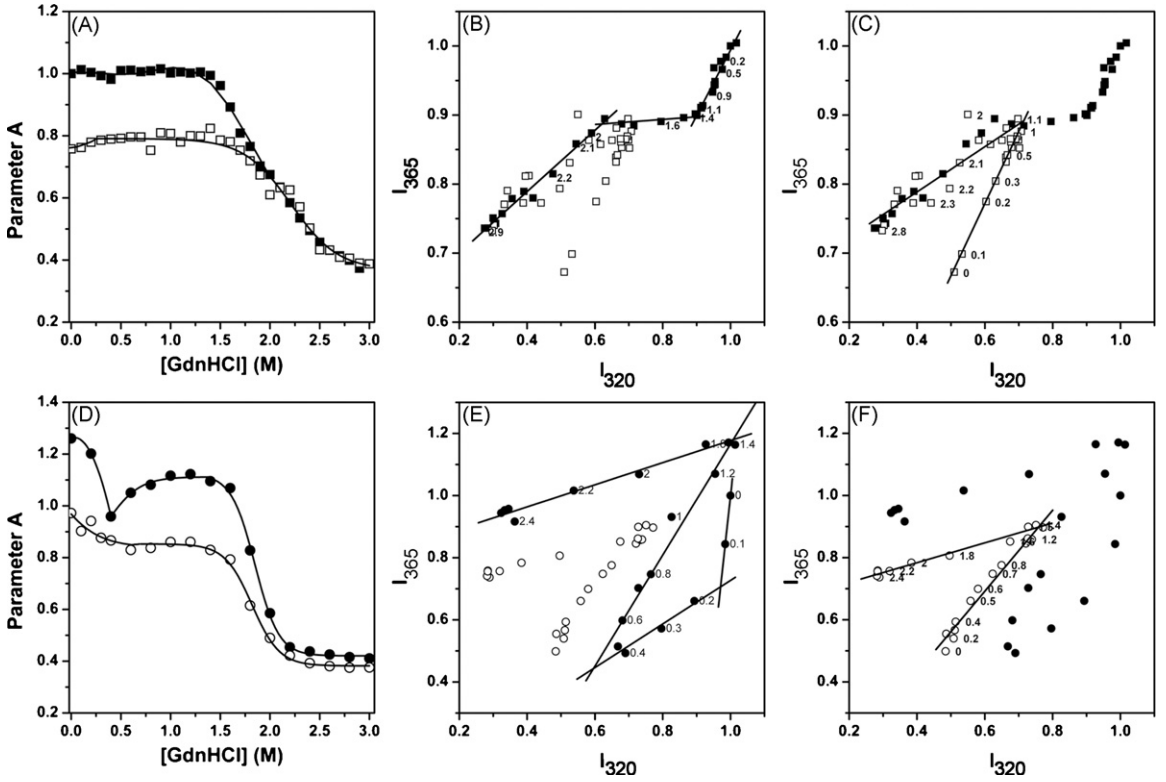

Fig. 7. Parameter A (A and D) and phase diagram analysis (B, C, E, and F) of the unfolding (filled squares and circles) and refolding (open squares and circles) of the wild type (A–C) and P237H (D–F) HCA II. The data were from those in Fig. 6. Parameter A is the quotient of the Trp fluorescence intensity at 320 nm (I_{320}) to that at 365 nm (I_{365}). The phase diagrams were constructed by plotting I_{365} vs. I_{320}. The I_{320} and I_{365} data were normalized by the intensities at 320 and 365 nm of the Trp fluorescence of the samples in the absence of GdnHCl, respectively. In the phase diagrams, concentrations of GdnHCl are labeled next to the corresponding symbols, and each straight line represents an all-or-none transition between two conformers.

which suggested that the folding of the mutant was irreversible. The differences between the WT and mutated protein also suggested that the P237H mutation might alter the folding pathway of HCA II. Unlike the sigmoidal unfolding transition of the WT, the parameter A of the mutant dropped quickly as GdnHCl concentrations increased to 0.4 M, then increased to a plateau, and finally decreased to a level similar to the fully-unfolded WT protein. This complex process suggested that at least two different intermediates, populated at around 0.4 and 1.5 M GdnHCl, might be involved in the unfolding of the P237H HCA II. However, the intermediate at 0.4 M GdnHCl was not observed in the refolding process, which suggested that the refolding pathway of the mutant was different from the unfolding pathway.

To more precisely identify the effects of P237H mutation on the HCA II folding pathway, phase diagram analysis, which has been shown to be a powerful and precise tool in the characterization of folding intermediates (Bushmarina et al., 2001), was used for the construction of the phase diagrams of the Trp fluorescence spectra for the WT and mutated protein (Fig. 7). In general, the phase diagram reflects the correlation of fluorescence between two fluorescence wavelengths (usually 320 and 365 nm). For a two-state process, the intensity of the two wavelengths changes linearly and a straight line can be observed in the phase diagram. For a multi-state process, several lines can be found in the diagram and each line reflects a two-state process. The joint point of two adjacent lines indicates that a folding intermediate is populated. The folding of CA has been thoroughly studied by phase diagram analysis previously (Bushmarina et al., 2001). As shown in Fig. 7B, three linear regions could be identified in the unfolding profile of the WT HCA II, which suggested that two unfolding intermediates, which were populated at 1.4 and 1.8 M GdnHCl, were involved in the unfolding of the WT protein. Only one refolding intermediate populated at 1.1 M GdnHCl could be identified in the refolding profile of the WT HCA II. The curves of unfolding and refolding of the WT enzyme were not overlapped at GdnHCl concentrations lower than 1.1 M, which confirmed our previous

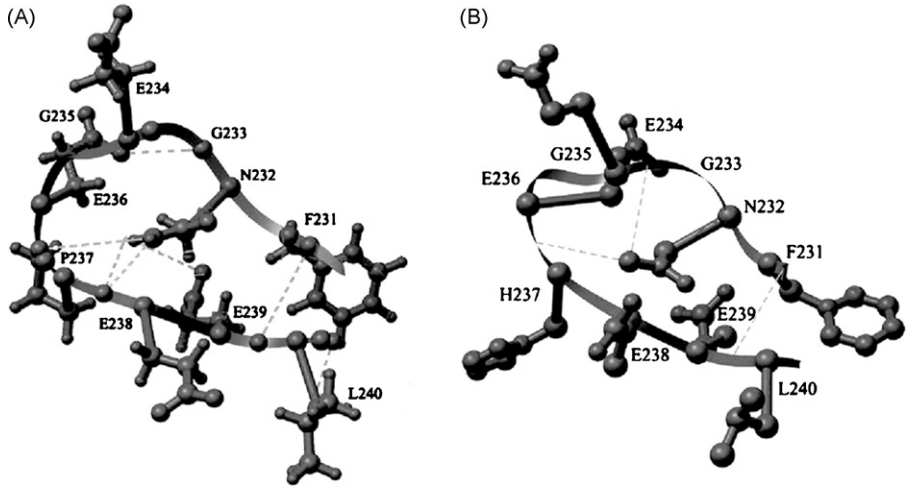

Fig. 8. Modeled structures of (A) HCA II and (B) HCA II_{P237H} in the vicinity of residue 237. The structures were generated through molecular modeling using the 2CBA structure as described in Section 2. Hydrogen bonds are indicated by broken lines.

deduction that the folding of WT HCA II was not fully reversible under our conditions. Interestingly, four linear regions could be identified in the unfolding diagram of P237H HCA II, indicating the occurrence of three intermediates (populated at 0.2, 0.4 and 1.4 M GdnHCl) in the unfolding pathway. Similar to the refolding of the WT protein, only one refolding intermediate populated at 1.4 M GdnHCl concentration could be identified for the mutated protein. The different refolding and unfolding profiles also indicated that the folding of P237H HCA II was irreversible.

3.5. Molecular modeling

To further elucidate the structural basis of the spectroscopic results, molecular modeling of the structure of the mutated protein was carried out using the crystal structure of HCA II (Hakansson et al., 1992) as a starting template. As shown in Fig. 8, the P237H mutation resulted in significant changes of the hydrogen bonding network in the loop region where P237 is located. Four hydrogen bonds in WT HCAII were found to be lost because of the mutation: the hydrogen bonds between N232 and E238, between N232 and E239, between G233 and E235, and the one between F231 and L240. These hydrogen bonds are crucial to maintain the structure and stability of the loop region and the turn around P237 in WT HCA II. It seems that the mutation removed the steric local constraints of P237, and the relative large side-chain volume of His led to the movement of the neighboring residues to avoid the unfavorable van der Waals contacts. The rearranged hydrogen bonding networks introduced more flexibility of the loop region, and thus made the loop more susceptible to destabilization by environmental stresses (heat or denaturants) compared with the WT enzyme.

4. Discussion

The effects of the single point mutations on protein structure and folding have been extensively studied, and the mutation of the buried non-polar residues is expected to be the most deleterious to protein structure and folding (Matthews, 1995). The residues located on the surface of a protein, particularly those in flexible loops, are thought to contribute little to the overall stability and folding of proteins. HCA II contains 15 *trans*- and 2 *cis*-prolines (residues 30 and 202) (Eriksson, Jones, & Liljas, 1988), among which P237 is located on the long loop close to the C-terminus (Hakansson et al., 1992) and does not participate in the catalysis (Lesburg & Christianson, 1995), nor the initial folding nucleus or the rate-limiting proline isomerization step during refolding (Tweedy, Nair, Paterno, Fierke, & Christianson, 1993). Interestingly, in this research it was found that the single point mutation P237H not only destabilized the native conformation, but also affected the folding pathway of HCA II.

As CA is a model protein, its folding has been thoroughly studied and found to be a multi-state process (Bushmarina et al., 2001; Cleland & Wang, 1990; Henkens et al., 1982; Semisotnov et al., 1990; Wong & Tanford, 1973). The results of the WT HCA II herein were quite consistent with those of previous investigations. As for the unfolding of P237H HCA II, a

dramatically wide plateau (from 0.4 to 1.5 M GdnHCl) appeared in the E_{max} profile of the intrinsic Trp fluorescence. Further analysis by parameter A and phase diagram indicated that there were three unfolding intermediates, populated at GdnHCl concentrations of 0.2 (I^U_1), 0.4 (I^U_2) and 1.4 M (I^U_3), respectively. Thus the wide plateau in the E_{max} profile of Trp fluorescence might be the apparent result of the population of the I^U_2 and I^U_3. Considering that P237H mutation only caused a slight decrease (about 30%) of the Gibbs free energy ΔG_{IU}° (Table 1) and the ANS intensity reached its maximum at about 1.2 M GdnHCl (Fig. 6), I^U_3 might be a molten globular intermediate similar to the one that appeared in the unfolding of the WT HCA II. However, it seems that I^U_3 was somewhat more unstable than the molten globular intermediate of the WT protein since the transition from I^U_3 to the unfolded state was very steep (Fig. 6).

A low concentration of GdnHCl could effectively inactivate P237H HCA II and lead to the accumulation of two intermediates I^U_1 and I^U_2. The mutated enzyme could only retain ~15% of its activity at a GdnHCl concentration of 0.2 M and was fully inactivated at 0.4 M GdnHCl (Fig. 4). It seems that the intermediate I^U_1 was a native-like intermediate, which had limited Trp exposure to water and similar hydrophobic exposure to the native state. The major difference between I^U_1 and the native state was the activity. The intermediate I^U_2 was fully inactivated, with a similar extent of exposed Trp to I^U_3 and a slight increase of hydrophobic exposure. The occurrence of I^U_1 and I^U_2 at low concentrations of GdnHCl suggested that P237H HCA II was only marginally stable. This conclusion was further confirmed by the low Gibbs free energy ΔG_{NI}° (about 0.5 kcal/mol) for the mutated protein. The small discrepancy of the free energy between the native state, I^U_1 and I^U_2, might make it difficult for the protein to reach the native state kinetically. More importantly, the accumulation of the misfolded species could also have resulted in the appearance of off-pathway aggregates in the *in vitro* refolding experiments (Fig. 5) and the formation of large amounts of inclusion bodies when expressed in *E. coli*.

It is worth noting that the P237H mutation did not significantly affect the enzymatic parameters of HCA II. The results herein suggested that the mutation might mainly impair the structure and stability of the enzyme. However, the effects of P237H mutation did not cause more hydrophobic exposure of the protein, but induced more Trp residues exposed to water and less dispersed NMR signals (Fig. 3). The results in Fig. 3 suggested that the P237H mutation might have caused a modification of the local structures, which allowed the easy entry of water molecules into the interior of the molecule. The structure of HCA II (Hakansson et al., 1992) indicates that there exist hydrogen networks between the segments 230–233 and 236–239, where P237 is a major residue forming the turn structure. The mutation from steric Pro to His might disrupt the local hydrogen networks and thus destabilize the C-terminal segment of HCA II (Fig. 8). Previous studies have shown that the refolding of the unique trefoil knot in the C-terminus is one of the slowest steps during CA refolding, and the refolding of this region is accompanied with the recovery of activity (Fransson et al., 1992; Freskgard, Carlsson, Martensson, & Jonsson, 1991). The incorrect knot topology of the C-terminal dramatically affects the formation of the active site and decreases the mechanical strength of the enzyme (Alam, Yamada, Carlsson, & Ikaia, 2002). In this research, it was also found that P237H HCA II was less stable than the WT enzyme (Figs. 4 and 6), and could not recover its activity when refolded *in vitro* (data not shown). Moreover, the formation of the molten globular refolding intermediate (I^U_3) was not significantly affected by the mutation (Fig. 6 and Table 1). Thus it seems more likely that the P237H mutation impaired the final correct positioning of the C-terminal segments during the refolding from I^U_3 to the native state.

Although P237H HCA II was not able to regain its activity *in vitro*, small amounts of soluble proteins could be obtained when expressed in *E. coli*. Considering the effects of potential chaperones and crowding reagents, mutated proteins might be able to gain their native-like structure when folding *in vivo* (Dobson, 2003; Rutherford & Lindquist, 1998). Further research on the role of crowding reagents in P237H HCA II refolding will be very interesting. It is interesting that the mutated enzyme had the same pH adaptation as the WT HCA II, which might be important to its cellular function of maintaining the acid–base equilibrium. However, since the loss-of-function mutation in patients was a hybrid and half of the normal levels of HCA II was enough to maintain the cell functions (Aramaki et al., 1993; Sly, 1991), it is unclear yet whether P237H HCA II could cause any abnormality (folding diseases) in cells. Nevertheless, the results in this research suggested that the correct positioning of the long loop around P237 might be crucial to the folding of HCA II, and particularly to the formation of the active site.

Acknowledgements

This investigation was supported by Grants 30500084 (to Y.-B. Yan) and 30221003 (to H.-M. Zhou) from

the National Natural Science Foundation of China, and Grant 101023 from the Fok Ying Tong Education Foundation (to Y.-B. Yan).

References

Alam, M. T., Yamada, T., Carlsson, U., & Ikaia, A. (2002). The importance of being knotted: effects of the C-terminal knot structure on enzymatic and mechanical properties of bovine carbonic anhydrase II. *FEBS Lett.*, *519*, 35–40.

Almstedt, K., Lundqvist, M., Carlsson, J., Karlsson, M., Persson, B., Jonsson, B.-H., Carlsson, U., & Hammarstrom, P. (2004). Unfolding a folding disease: Folding, misfolding and aggregation of the marble brain syndrome-associated mutant H107Y of human carbonic anhydrase II. *J. Mol. Biol.*, *342*, 619–633.

Anfinsen, C. B. (1973). Principles that govern the folding of protein chains. *Science*, *181*, 223–230.

Aramaki, S., Yoshida, I., Yoshino, M., Kondo, M., Sato, Y., Noda, K., Jo, R., Okue, A., Sai, N., & Yamashita, F. (1993). Carbonic anhydrase II deficiency in three unrelated Japanese patients. *J. Inher. Metab. Dis.*, *16*, 982–990.

Borthwick, K. J., Kandemir, N., Topaloglu, R., Kornak, U., Bakkaloglu, A., Yordam, N., Ozen, S., Mocan, H., Shah, G. N., Sly, W. S., & Karet, F. E. (2003). A phenocopy of CAII deficiency: a novel genetic explanation for inherited infantile osteopetrosis with distal renal tubular acidosis. *J. Med. Genet.*, *40*, 115–121.

Bushmarina, N. A., Kuznetsova, I. M., Biktashev, A. G., Turoverov, K. K., & Uversky, V. N. (2001). Partially folded conformations in the folding pathway of bovine carbonic anhydrase II: A fluorescence spectroscopic analysis. *Chembiochemistry*, *2*, 813–821.

Cleland, J. L., & Wang, D. I. (1990). Refolding and aggregation of bovine carbonic anhydrase B: quasi-elastic light scattering analysis. *Biochemistry*, *29*, 11072–11078.

Dobson, C. M. (2001). The structural basis of protein folding and its links with human disease. *Phil. Trans. R. Soc. Lond. B*, *356*, 133–145.

Dobson, C. M. (2003). Protein folding and misfolding. *Nature*, *426*, 884–890.

Dodgson, S. J., Tashian, R. E., Gross, G., & Carter, N. D. (1991). *The carbonic anhydrases: Cellular physiology and molecular genetics*. New York: Plenum.

Eriksson, A. E., Jones, T. A., & Liljas, A. (1988). Refined structure of bovine carbonic anhydrase II at 2.0 Å resolution. *Proteins*, *4*, 274–282.

Feng, S., Zhao, T.-J., Zhou, H.-M., & Yan, Y.-B. (2007). Effects of the single point genetic mutation D54G on muscle creatine kinase activity, structure and stability. *Int. J. Biochem. Cell Biol.*, *39*, 392–401.

Francis, P. J., Berry, V., Moore, A. T., & Bhattacharya, S. (1999). Lens biology: Development and human cataractogenesis. *Trends Genet.*, *15*, 191–196.

Fransson, C., Freskgard, P. O., Herbertsson, H., Johansson, A., Jonasson, P., Martensson, L. G., Svensson, M., Jonsson, B. H., & Carlsson, U. (1992). *cis–trans* isomerization is rate-determining in the reactivation of denatured human carbonic anhydrase II as evidenced by proline isomerase. *FEBS Lett.*, *296*, 90–94.

Freskgard, P. O., Carlsson, U., Martensson, L. G., & Jonsson, B. H. (1991). Folding around the C-terminus of human carbonic anhydrase II. Kinetic characterization by use of a chemically reactive SH-group introduced by protein engineering. *FEBS Lett.*, *289*, 117–122.

Hakansson, K., Carlsson, M., Svensson, L. A., & Liljas, A. (1992). Structure of native and apo carbonic anhydrase II and structure of some of its anion-ligand complexes. *J. Mol. Biol.*, *227*, 1192–1204.

Henkens, R. W., Kitchell, B. B., Lottich, S. C., Stein, P., & Williams, T. J. (1982). Detection and characterization using circular dichroism and fluorescence spectroscopy of a stable intermediate conformation formed in the denaturation of bovine carbonic anhydrase with guanidinium chloride. *Biochemistry*, *21*, 5918–5923.

Hu, P. Y., Lim, E. J., Ciccolella, J., Strisciuglio, P., & Sly, W. S. (1997). Seven novel mutations in carbonic anhydrase II deficiency syndrome identified by SSCP and direct sequencing analysis. *Hum. Mutat.*, *9*, 383–387.

Jiang, Y., Yan, Y.-B., & Zhou, H.-M. (2006). Polyvinylpyrrolidone 40 assists the refolding of bovine carbonic anhydrase B by accelerating the refolding of the first molten globule intermediate. *J. Biol. Chem.*, *281*, 9058–9065.

Jones, G. L., & Shaw, D. C. (1983). A chemical and enzymological comparison of the common major human erythrocyte carbonic anhydrase II, its minor component, and a new genetic variant CA II Melbourne (237 Pro leads to His). *Hum. Genet.*, *63*, 392–399.

Jones, G. L., Sofro, A. S. M., & Shaw, D. C. (1982). Chemical and enzymological characterization of an Indonesian variant of human erythrocyte carbonic anhydrase II CAII^{Jogjakarta} (17Lys→Glu). *Biochem. Genet.*, *20*, 979–1000.

Lesburg, C. A., & Christianson, D. W. (1995). X-ray crystallographic studies of engineered hydrogen bond networks in a protein-zinc binding site. *J. Am. Chem. Soc.*, *117*, 6838–6844.

Lin, K.-T. D., & Deutsch, H. F. (1972). Human carbonic anhydrases. VIII. Isolation and characterization of a polymorphic form of a C type isozyme. *J. Biol. Chem.*, *247*, 3761–3766.

Lindskog, S. (1997). Structure and mechanism of carbonic anhydrase. *Pharmacol. Ther.*, *74*, 1–20.

Matthews, B. W. (1995). Studies on protein stability with T4 lysozyme. *Adv. Protein Chem.*, *46*, 249–278.

Pocker, Y., & Stone, J. T. (1967). The catalytic versatility of erythrocyte carbonic anhydrase. III. Kinetic studies of the enzyme-catalyzed hydrolysis of *p*-nitrophenyl acetate. *Biochemistry*, *6*, 668–678.

Roth, D. E., Venta, P. I., Tashian, R. E., & Sly, W. S. (1992). Molecular basis of human carbonic anhydrase II deficiency. *Proc. Natl. Acad. Sci. U.S.A.*, *89*, 1804–1808.

Rutherford, S. L., & Lindquist, S. (1998). Hsp90 as a capacitor for morphological evolution. *Nature*, *396*, 336–342.

Santoro, M. M., & Bolen, D. W. (1988). Unfolding free energy changes determined by the linear extrapolation method. 1. Unfolding of phenylmethanesulfonyl alpha-chymotrypsin using different denaturants. *Biochemistry*, *27*, 8063–8068.

Semisotnov, G. V., Uversky, V. N., Sololovsky, I. V., Gutin, A. M., Razgulyaev, O. I., & Rodionova, N. A. (1990). Two slow stages in refolding of bovine carbonic anhydrase B are due to proline isomerization. *J. Mol. Biol.*, *213*, 561–568.

Sly, W. S. (1991). Carbonic anhydrase II deficiency syndrome: clinical delineation, interpretation and implications. In S. J. Dodgson, R. E. Tashian, G. Gros, & N. D. Carter (Eds.), *The carbonic anhydrases: Cellular physiology and molecular genetics* (pp. 183–193). New York: Plenum Press.

Sly, W. S., Hewett-Emmett, D., Whyte, M. P., Yu, Y.-S. L., & Tashian, R. E. (1983). Carbonic anhydrase II deficiency identified as the primary defect in the autosomal recessive syndrome of osteopetrosis with renal tubular acidosis and cerebral calcification. *Proc. Nat. Acad. Sci. U.S.A.*, *80*, 2752–2756.

Sly, W. S., & Hu, P. Y. (1995). Human carbonic anhydrases and carbonic anhydrase deficiencies. *Annu. Rev. Biochem.*, *64*, 375–401.

Sly, W. S., Lang, R., Avioli, L., Haddad, J., Lubowitz, H., & McAlister, W. (1972). Recessive osteopetrosis: New clinical phenotype. *Am. J. Hum. Genet.*, *24*, 34A.

Soda, H., Yukizane, S., Yoshida, I., Aramaki, S., & Kato, H. (1995). Carbonic anhydrase II deficiency in a Japanese patient produced by a nonsense mutation (TAT→TAG) at Tyr-40 in exon 2 (Y40X). *Hum. Mutat.*, *5*, 348–350.

Su, J.-T., Kim, S.-H., & Yan, Y.-B. (2007). Dissecting the pre-transitional conformational changes in aminoacylase I thermal denaturation. *Biophys. J.*, *92*, 578–587.

Stefani, M., & Dobson, C. M. (2003). Protein aggregation and aggregate toxicity: new insights into protein folding, misfolding diseases and biological evolution. *J. Mol. Med.*, *81*, 678–699.

Turoverov, K. K., Haitlina, S. Y., & Pinaev, G. P. (1976). Ultra-violet fluorescence of actin. Determination of actin content in actin preparations. *FEBS Lett.*, *62*, 4–6.

Tweedy, N. B., Nair, S. K., Paterno, S. A., Fierke, C. A., & Christianson, D. W. (1993). Structure and energetics of a nonproline *cis*-peptidyl linkage in a proline-202→alanine carbonic anhydrase II variant. *Biochemistry*, *32*, 10944–10949.

Venta, P. J., Welty, R. J., Johnson, T. M., Sly, W. S., & Tashian, R. E. (1991). Carbonic anhydrase II deficiency syndrome in a Belgian family is caused by a point mutation at an invariant histidine residue (107 His→Tyr): complete structure of the normal human CA II gene. *Am. J. Hum. Genet.*, *49*, 1082–1090.

Wetlaufer, D. B., & Xie, Y. (1995). Control of aggregation in protein refolding: A variety of surfactants promote renaturation of carbonic anhydrase II. *Protein Sci.*, *4*, 1535–1543.

Wong, K. P., & Tanford, C. (1973). Denaturation of bovine carbonic anhydrase B by guanidine hydrochloride. A process involving separable sequential conformational transitions. *J. Biol. Chem.*, *248*, 8518–8523.